Biochimica et Biophysica Acta 1838 (2014) 3088–3096

Contents lists available at ScienceDirect

Biochimica et Biophysica Acta

journal homepage: www.elsevier.com/locate/bbamem

Epileptic seizures induce structural and functional alterations on brain tissue membranes

Sevgi Turker [a,d], Mete Severcan [b], Gul Ilbay [c], Feride Severcan [d,*]

[a] Department of Biology, Kocaeli University, 41300 Kocaeli, Turkey
[b] Department of Electrical and Electronics Engineering, Middle East Technical University, 06800 Ankara, Turkey
[c] Department of Physiology, Medical School of Kocaeli University, 41300 Kocaeli, Turkey
[d] Department of Biological Sciences, Middle East Technical University, 06800 Ankara, Turkey

ARTICLE INFO

Article history:
Received 15 April 2014
Received in revised form 9 August 2014
Accepted 23 August 2014
Available online 3 September 2014

Keywords:
PTZ
Audiogenetically susceptible WAG/Rij rat
FT-IR spectroscopy
Brain tissue membrane
Neural network
PCA

ABSTRACT

Epilepsy is characterized by disruption of balance between cerebral excitation and inhibition, leading to recurrent and unprovoked convulsions. Studies are still underway to understand mechanisms lying epileptic seizures with the aim of improving treatment strategies. In this context, the research on brain tissue membranes gains importance for generation of epileptic activities. In order to provide additional information for this field, we have investigated the effects of pentylenetetrazol-induced and audiogenetically susceptible epileptic seizures on structure, content and function of rat brain membrane components using Fourier transform infrared (FT-IR) spectroscopy. The findings have shown that both two types of epileptic seizures stimulate the variations in the molecular organization of membrane lipids, which have potential to influence the structures in connection with functions of membrane proteins. Moreover, less fluid lipid structure and a decline in content of lipids obtained from the ratio of CH_3 asym/lipid, CH_2 asym/lipid, C═O/lipid, and olefinic═CH/lipid and the areas of the PO_2 symmetric and asymmetric modes were observed. Moreover, based on IR data the changes in the conformation of proteins were predicted by neural network (NN) analysis, and displayed as an increase in random coil despite a decrease in beta sheet. Depending on spectral parameters, we have successfully differentiated treated samples from the control by principal component analysis (PCA) and cluster analysis.
In summary, FT-IR spectroscopy may offer promising attempt to identify compositional, structural and functional alterations in brain tissue membranes resulting from epileptic activities.

1. Introduction

Epilepsy is a heterogeneous collection of neurological disorders that have common recurrent hypersynchronous activation of neurons in focal areas or in the whole brain [1]. Even though epilepsy is a clinically well-known neurological disorder, there is no single treatment strategy to prevent epileptic conditions. To accomplish new advances for this concept, the identification of seizure-induced changes correlating with their pathology has been aimed in most of the studies [2]. However, the research in human needs invasive intervention, therefore; various animal models have been developed.

Pentylenetetrazol (PTZ)-treated animal models have been widely used in epilepsy research. Single and repeated injection of PTZ causes generalized tonic–clonic seizures, which result in similar alterations observed in human epilepsy [3]. Another model includes a subpopulation of some WAG/Rij (Wistar albino Glaxo from Rijswijk) rats, which are susceptible to audiogenic (convulsive) seizures. In response to audiogenic stimulation WAG/Rij rats show motor seizures involving wild running followed by clonic convulsion and/or catalepsy. Since they display a dual pathology (coexistence of nonconvulsive and convulsive seizures), such pattern offers mixed form of epileptic model [4].

Fourier transform infrared (FT-IR) spectroscopy has the ability to investigate the composition, structure and function of biomolecules, to detect the changes in these parameters induced by any pathological condition [5–15]. Therefore, over the years, this method has been widely addressed for identification of disease-conditions in various biological samples such as isolated membranes and their constituent lipids [6,11,12]. However, its application in epilepsy and epileptic conditions is scarce with limited number of reports. We previously investigated the effects of pentylenetetrazol-induced seizures on whole rat brain by FT-IR spectroscopy [15]. In other studies, synchrotron radiation Fourier transform infrared (SRFT-IR) micro-spectroscopy was applied for analysis of whole rat brain tissue [16] and hippocampus [17] as well as for examination of accumulated creatine in hippocampus [18] upon pilocarpine-evoked epilepsy. The effects of epileptic seizures on rat femur and tibia bone tissue were also detected by FT-IR microspectroscopy [19]. Kumar, et al. [20] reported the pathological changes in the IgG samples taken from people suffering from epilepsy by using the same technique.

* Corresponding author. Tel.: +90 312 210 51 66; fax: +90 312 210 79 76.
E-mail address: feride@metu.edu.tr (F. Severcan).

http://dx.doi.org/10.1016/j.bbamem.2014.08.025
0005-2736/

It has been well-documented that proper function of membrane is largely correlated with its structure. And, membrane structure is fully mediated through physical properties of fatty acids, polar head groups of lipid membrane proteins, as well as lipid order, lipid fluidity and content of membrane components [21]. When brain tissue membrane functions are considered, the determination of seizure-stimulated changes on brain tissue membranes has great importance in understanding the generation of epileptic conditions. This was suggested by previous studies focusing on alterations induced by epileptic seizures on subcellular membrane compartments such as mitochondrial, lysosomal and microsomal membranes [22–24]. Under the light of such background, the aim of the study is concerned with the role of membrane structure and function in development of non-spontaneous PTZ-induced and audiogenetically susceptible seizures. We designed our experiment to investigate acute effects of epileptic seizures on membrane compartments, all of which may have potential role to generate epileptogenesis.

For this purpose, we used Fourier transform infrared (FT-IR) spectroscopy. Although FT-IR spectroscopy gives global information about lipids and proteins rather than providing information about specific types of lipids and proteins, it is an effective technique to study disease-induced early compositional and structural alterations rapidly and sensitively without need for isolation of particular biomolecules [5–15]. We have also predicted the structural changes in membrane proteins using neural networks (NNs) based on FT-IR spectral data as previously used [15,25]. Finally, both principal component analysis (PCA) and cluster analysis have been performed to discriminate treated groups from the control, based on their spectral variations.

2. Experimental

2.1. Chemicals

All chemicals were used without further purification. PTZ, sucrose, trizma base, ethylene diamine tetra acetic acid (EDTA), phenylmethylsulfonylfluoride (PMSF), buthylatedhyroxytoluene, magnesium chloride, pepstatin, and aprotonin were purchased from Sigma (Sigma Chemical Co., St. Louis, MO, USA). Trichloroacetic acid and hydrochloric acid were obtained from Merck.

2.2. Animal studies

All procedures were performed in accordance with welfare guidelines approved by Ethics Committee (KOU-44543) and all treatment processes were applied by following the literature.

Adult male Wistar rats weighing 200–250 g were housed in a room under a constant 12-h light/dark cycle with humidity of 10–50% having free access to standard rat food and tap water. Three groups as control ($n = 6$), PTZ-induced ($n = 6$) and audiogenetically susceptible group ($n = 5$) were designed. All animals were treated once a day for five days. After each injection, the monitored seizures were scored based on literature, for both treated groups [26,27]. Since all animals come from the same strain of Wistar rats, only one group of control consisting of wild type Wistar rats was used as carried out in earlier studies [26]. This group received intraperitoneal (i.p.) physiological saline and key ringing and, no epileptic seizure was observed. The PTZ-group was intraperitoneally injected by convulsant dose (60 mg/kg) once a day. PTZ-induced convulsions were scored according to Racine 26] as follows: stage 0; no response, stage 1; ear and facial twitching, stage 2; convulsive waves through the body, stage 3; myclonic jerks, stage 4; clonic–tonic seizures, and stage 5; generalized clonic–tonic seizures. For the entire PTZ-group, the seizures were interpreted as 4.2 ± 0.3, which reflects stage 4 and stage 5, and lasted 400 ± 30 s. To induce audiogenetically susceptible seizures, audiogenetically susceptible WAG/Rij rats were placed in a testing chamber and sound stimulation was provided by a short manual shake of a bunch of keys (6–10 metal door keys on a metal key-ring) held at 50 cm above the floor of the box. The frequency and intensity of the sound were measured by Biopac MP36 Data Acquistion System (St Barbara, CA,USA) and by sound level meters Lutron SL-4012 (Taipei, Taiwan). The peak frequency of sound stimulation was approximately 6.7 kHz with a wide range of 2–14 kHz. The intensity of sound ranged from 80 to 90 dB. Upon this stimulus, several phases of seizures occur. The intensity of audiogenic seizures was estimated with four level scale as proposed by Krushinski and Molodkina [28]. Stage 0; lack of audiogenic seizures, 1; wild running, 2; clonic seizures with the rat lying "on its" belly, 3; continuation of clonic seizures with the animal turning on its side, and 4; end of seizures with tonic phase. The seizures were scored as 3.2 ± 0.6 and lasted 79 ± 5 s. Subsequently, at the end of five days following the observation of the last seizure, the animals were sacrificed for FT-IR spectroscopic study, and the brains were quickly dissected out.

2.3. Sample preparation for FT-IR study

For the isolation of plasma membrane from rat brain, a method optimized by Scott and co-workers [29] was followed. The solutions were prepared in advance:

(A) 0.25 M sucrose, 10 mM Tris–HCl, 1 mM $MgCl_2$, pH 7.4, density 1.03 g/mL (1.3450)
(B) 0.25 M sucrose, density 1.03 g/mL (1.3450)
(C) 2.0 M sucrose, 10 mM Tris–HCl, 1 mM $MgCl_2$ pH 7.4, density 1.26 g/mL (1.4297)

Briefly, each brain tissue was chopped in Reagent A containing pepstatin, aprotinin and PMSF and homogenized with a tissue homogenizer using a loose-fitting Teflon pestle. Then, 10,000 lbs pressure to homogenate was applied by French pressure cell (Thermo, Electron). After filtration, the homogenate was diluted with Reagent A, and centrifuged for 10 min at 300 $\times g$ and 0–2 °C. The supernatant was collected and pellet was resuspended in Reagent A, then, it was centrifuged again. The supernatants from two extractions were pooled and centrifuged for 15 min at 1500 $\times g$, 0–2 °C. The resulting supernatant was resuspended in Reagent A and was homogenized by 10-second strokes of the loose-fitting pestle. Then, suspension volume was increased using Reagent C, transferred to a centrifuge tube, and carefully overlaid with 4 mL of Reagent B. Afterwards, the sample was centrifuged at 104,000 $\times g$ for a max of 75 min at 2 °C. Membrane structures, which formed a layer at the interface, were collected and resuspended in Reagent B and homogenized as before with strokes of the loose-fitting pestle. Finally, the membrane fractions were centrifuged at 1500 $\times g$ for 20 min. The resulting pellet was resuspended in Reagent B and manually homogenized using Teflon glass homogenizer. The suspension was composed of the membranes originating from various membrane components. This membrane preparation was stored at −80 °C till FT-IR study.

2.4. FT-IR spectroscopic study

IR spectra were acquired using Perkin Elmer Spectrum 100 FT-IR spectrometer (Perkin Elmer, Norwalk, CT, USA) equipped with a deuterated triglycine sulfate (DTGS) detector. The samples were continuously purged with dry air. The interference of atmospheric water vapor and carbon dioxide was automatically removed by subtraction of background from the sample spectra. To obtain the best quality spectrum, scanning parameters were optimized by following the earlier studies with mammalian tissue samples [6,12,15,25,30]. 15 μL samples were placed between ZnSe windows with a spacer to obtain 12 μm sample thickness. All spectra were recorded at the wavenumber range of 4000–900 cm^{-1}. Interferograms were averaged for 200 scans at 2 cm^{-1} resolution at 25 °C. For each scan, the spectra of three independent aliquots from the same sample were recorded to minimize any variability, and to check the precision of the absorbance values. These replicates belonging to the same source

were averaged to represent the spectrum of each animal. The final average spectrum was then used for data evaluation and statistical analysis.

The water absorption bands overlap the modes of proteins (1700–1500 cm^{-1}) and lipids (3050–2800 cm^{-1}), therefore; the buffer (containing Tris–HCl, $MgCl_2$ and PMSF) spectrum was subtracted from each spectrum using Perkin Elmer Spectrum One software as described by our group [6,15,25] and others [30,31]. The wavenumber values were measured as the center of weight of the peak. The bandwidth values were calculated as width measured at a 0.80 fraction of the absorption in terms of cm^{-1}.

For visual demonstration of the spectral differences among groups, baseline correction and normalization were carried out by the same software. For normalization process, the earlier studies [6–9,15,25,32] were followed and min–max normalization was applied. The linear baseline correction was standardized with respect to 4000, 2750, 1800 and 1000 cm^{-1} base points.

2.5. Protein secondary structure prediction

Amide I band between 1700 and 1600 cm^{-1} resulting from proteins was evaluated for the analysis of their secondary structure. The neural networks (NNs) were first trained using a data set including FT-IR spectra of 18 water soluble proteins recorded in water applying the method described previously [33]. The secondary structures of these proteins were known from X-ray crystallographic analysis. Amide I band was preprocessed prior to NN analysis. Preprocessing involves normalization and discrete cosine transformation (DCT). To improve the training of the NNs, the size of the data set was increased by interpolating the available FT-IR spectra. NNs were trained using Bayesian regularization. For each structure parameter, a separate NN was trained whose number of inputs, i.e. the number of DCT coefficients, and number of hidden neurons were optimized. The trained NNs have standard error of prediction values of 4.19% for alpha-helix, 3.49% for beta-sheet and 3.15% for turns. The secondary structure parameters of the proteins were predicted by applying to the inputs of the trained NNs the preprocessed FT-IR data [33].

2.6. Principal component analysis (PCA)

Principal component analysis (PCA) program was kindly provided by Prof. Erik Goormaghtigh. Grouping of spectra into clusters and the extent to which these clusters correspond to classes of sample are derived within the regions between 3050 and 900 cm^{-1}, 3050 and 2800 cm^{-1} and 1700 and 1600 cm^{-1} utilizing the original absorption spectra. PCA offers two types of information: clustering and identification of variables among the groups. It is a statistical data reduction method that transforms the original spectra into a new set of uncorrelated eigenvectors. These components are independent from each other and listed in order according to how much of the original data variance is accounted for by each component. Thus, in PCA each spectrum appears as a single point in n-dimensional space, which represents the characteristic structure information of the data along different eigenvectors retaining as much of the information in the original variables as possible. This enables the spectra to be described as a function of specific properties, and not a function of intensities. The outcome of the analysis can be presented as scatter plots [8,32]. From the obtained plots, sensitivity and specificity parameters were calculated in different spectral ranges as performed in Severcan, et al. [14]. Briefly, negative (true and false) and positive values (true and false) were identified according to treated and control samples. The sensitivity measures the proportion of actual positives such as the percentage of treated rats defined as having disease; and the specificity measures the proportion of negatives such as the percentage of control rats, which do not have disease.

2.7. Cluster analysis

Hierarchial cluster analysis was performed on the second derivatives of all spectra using thirteen smoothing point Savitzky–Golay algorithm on the frequency range between 3050 and 900 cm^{-1}, 3050 and 2800 cm^{-1} and 1700 and 1600 cm^{-1}. The spectra were first vector normalized over the investigated frequency range and then Ward's algorithm was used to construct dendrograms by OPUS 5.5 (Bruker Optic, GmbH). The spectral distance was calculated between pairs of spectra as Pearson's product moment correlation coefficient [14,15]. Similarly to PCA, both specificity and sensitivity values were also calculated for each spectral region.

2.8. Statistical analysis

FT-IR spectral parameters and the results of NN predictions were compared by one-way ANOVA with Bonferroni correction in order to test the significance of the differences between the control and treated groups. The results with corrected p values were expressed as mean ± standard deviation. A p value of less than 0.05 was considered significant ($p < 0.05^*$, $p < 0.01^{**}$).

3. Results

Figs. 1 and 2 show normalized infrared spectra of control, PTZ-induced and audiogenetically susceptible groups of rat brain tissue membranes in the 3050–2800 cm^{-1} and 2000–900 cm^{-1} regions, respectively. The assignments of bands based on literature are given in Table 1. In Fig. 1, the spectra were normalized with respect to the CH_2 asymmetric stretching band at 2925 cm^{-1}, while the spectra were normalized with respect to Amide I band at 1645 cm^{-1} in Fig. 2. Numerical comparisons of band areas, frequencies, band area ratios and bandwidths are presented in Table 2. The difference in the spectral values between the control and treated groups appeared to be modest, but the alterations are consistent and statistically significant with marginal standard deviations. One feature of FT-IR spectroscopy, storage of acquired spectra in digitally encoded format, facilitates spectral interpretation with the aid of post-acquisition data manipulation algorithms. Such option provides the accurate detection of small changes even in weak absorption bands [5–7,9,15].

Statistical analysis revealed a significant ($p < 0.05^*$) decrease in the areas of the olefinic=CH (3015 cm^{-1}), the CH_2 asymmetric (2921 cm^{-1}), the C=O stretching (1736 cm^{-1}), the COO^- symmetric stretching (1400 cm^{-1}), the PO^-_2 asymmetric (1236 cm^{-1}) and the PO^-_2 symmetric stretching (1080 cm^{-1}) modes (Table 2). Additionally, detailed analysis of Amide I (1645 cm^{-1}) and Amide II (1540 cm^{-1}) absorptions showed significantly ($p < 0.05^*$) lowered area values for treated groups (Fig. 2 and Table 2). To minimize the probability of any artifact caused by variation in experimental conditions, the ratios of some specific modes (CH_3 asymmetric, CH_2 asymmetric, C=O stretching, olefinic=CH) to the lipid (the sum of the CH_2 asymmetric and symmetric stretching) were calculated. Lipid to protein ratio was measured by taking the ratio of lipid (the sum of the CH_2 asymmetric and symmetric stretching) to protein (the sum of the Amide I and Amide II). A significant ($p < 0.05^*$) increase in lipid to protein ratio, despite a decrease in CH_3 asym/lipid, CH_2 asym/lipid, C=O/lipid and olefinic=CH/lipid ratios were observed compared to control group (Table 2).

As illustrated in Fig. 2 and Table 2, the wavenumber values of the C=O, the PO^-_2 asymmetric and the PO^-_2 symmetric stretching modes of lipids significantly ($p < 0.05^*$) shifted to lower values.

Alterations in lipid order and fluidity can be determined by probing the vibrational modes in the C–H stretching region [5–9,15]. As shown in Table 2 and Fig. 2, two bandwidth values of CH_2 asymmetric and symmetric modes for audiogenetically susceptible group were significantly decreased ($p < 0.05^*$), while a slight variation for PTZ treated group

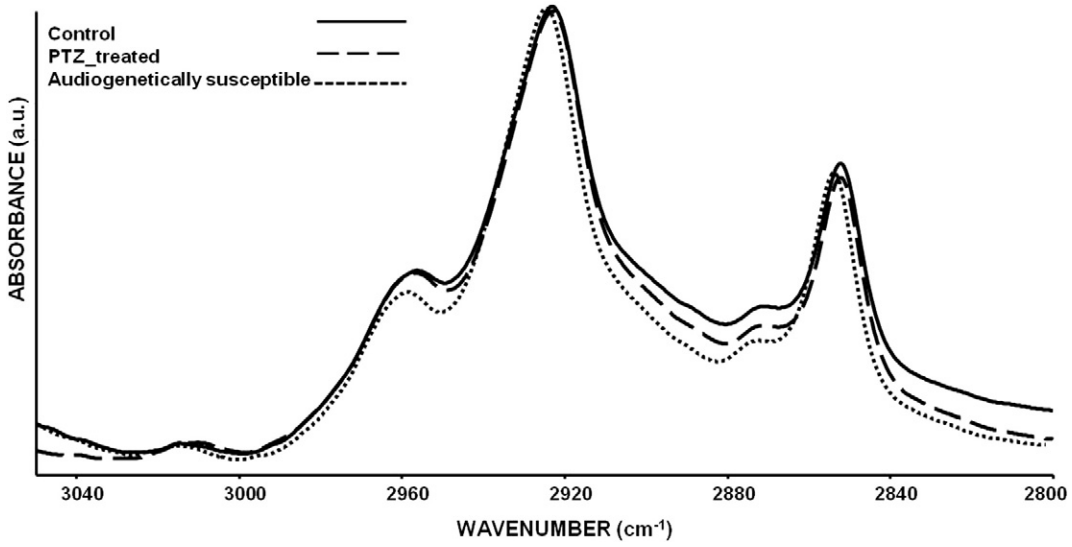

Fig. 1. Representative FT-IR spectra of control, PTZ-treated and audiogenetically susceptible groups in the region between 3050 and 2800 cm^{-1}. The spectra were normalized with respect to the CH_2 asymmetric stretching at 2925 cm^{-1}. The peaks in the spectra were assigned in Table 1.

was observed. The shift in these modes at 2922 cm^{-1} (CH_2 asymmetric) and 2851 cm^{-1} (CH_2 asymmetric) towards higher frequencies was significant ($p < 0.05^*$) only for audiogenetically susceptible group, but not for the PTZ-treated group.

The results of NN predictions, are presented in Fig. 3. A prominent increase ($p < 0.05^*$) in random coil and significant decrease ($p < 0.05^*$) in beta sheet structures were predicted, and a profound increment ($p < 0.05^*$) in alpha helix was estimated, only for audiogenetically susceptible group.

Fig. 4 demonstrates PCA and cluster analysis dendrogram based on the spectral differences in the regions 3050–900 cm^{-1}, 3050–2800 cm^{-1} and 1700–1600 cm^{-1}. As illustrated, control and treated groups were successfully discriminated with a high accuracy. PTZ-induced and audiogenetically susceptible groups displayed 100% specificity and 100% sensitivity values for all three different spectral regions.

4. Discussion

The communication of neurons is dependent on a balance between excitatory and inhibitory systems, therefore; the processes of neurotransmission are tightly regulated. Various presynaptic, synaptic, and postsynaptic elements control the communication between neurons in the multiple and complex neuronal networks. For example, under normal conditions neurons sense the presence of GABA and glutamate in the vicinity and it switches on special pumps on their membranes. Critically, the level can be disrupted in the case of membrane instability. In such cases, the pumps on membranes can no longer cope with the situation and both glutamate and c-aminobutyric acid (GABA) activities become dysfunctional [34]. This state is a display of imbalance between excitatory and inhibitory modes in neurotransmission. Concerning receptor–membrane interactions, both lipid and protein molecules distort

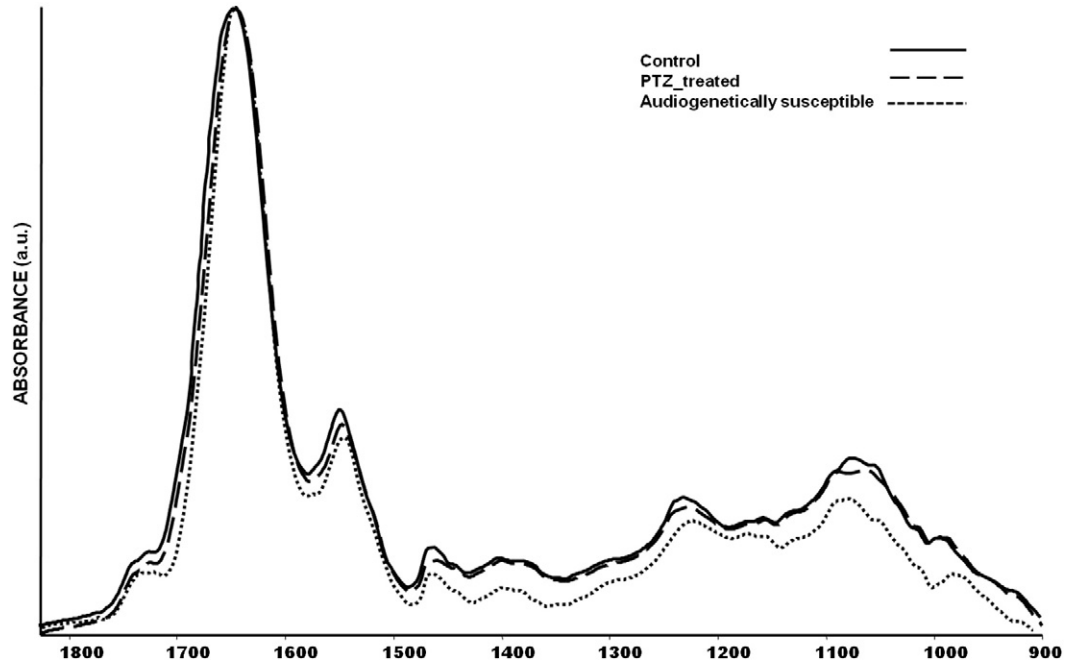

Fig. 2. Representative FT-IR spectra of control, PTZ-treated and audiogenetically susceptible groups in the region between 2000 and 900 cm^{-1}. The spectra were normalized with respect to the Amide I at 1645 cm^{-1}. The peaks in the spectra were assigned in Table 1.

Table 1
General band assignments of average FTIR spectrum of rat brain tissue membranes based on the literature.

No	Wavenumber (cm^{-1})	Definition of the spectral assignments
2	3012	HC═CH stretching: unsaturated lipids
3	2956	CH_3 asymmetric stretching: lipids and protein side chains
4	2925	CH_2 symmetric stretching: mainly lipids, with a little contribution from proteins
5	2870	CH_3 symmetric stretching: mainly protein side chains with a little contribution from lipids
6	2852	CH_2 symmetric stretching: mainly lipids, with a little contribution from lipids
7	1736	Saturated ester C═O stretch: phospholipids, cholesterol esters
8	1645	Amide I (mainly C═O stretch): proteins
9	1547	Amide II (C═N and N–H stretching): proteins
10	1400	COO^- symmetric stretching: fatty acids
11	1236	PO_2^- asymmetric stretching: phospholipids
12	1080	PO_2^- symmetric stretching: phospholipids

to provide the accessible sites for interaction, resulting in an effect on receptor and/or ion channel function by the structure of the surrounding lipid bilayer [35]. For instance, the structures adopted by the parts of a membrane protein that are located in the lipid head group region are determined, in part, by hydrogen bonding to the head groups. Taking into account that membrane lipids and proteins are strictly in contact, any variation in the ratio of these molecules such as unsaturated to unsaturated lipids and lipid to protein alters membrane thickness and curvature, which in turn affects lipid order and fluidity [6,36,37]. Fluidity and order parameters together with hydrophobic thickness of bilayer have prominent role in regulating many membrane functions, such as signal transduction, solute transport, and enzyme activity, associated with membranes [6,9,36]. Here, we investigated these parameters in order to obtain information about the presence of any disorder or disruption of membrane systems that might lead to their structural alterations, which show the imbalance between inhibitory and excitatory systems. All of these results are indications of structural alterations of membranes which in turn might cause conformational changes in receptors including GABA and glutamate.

Due to being the main components of membrane, any alteration in lipid content has a pivotal impact on membrane properties. It is worth noting again that IR spectroscopic technique lacks providing quantitative information particularly for a single type lipid and protein. However, in optical spectroscopy, according to Beer–Lambert law it is possible to use the intensity and/or, more accurately, the area of the absorption bands in order to obtain relative concentration information of the corresponding functional groups [5–9,15,38]. This has been previously confirmed by biochemical assays by us for lipid peroxidation products [15] and for proteins [8]. By utilizing this feature of FT-IR spectroscopy, in the current study we have evaluated areas and area ratios of lipid and protein modes.

The integrated area of the olefinic═CH band can be used as an index of relative concentration of double bonds in the lipid structure from unsaturated fatty acyl chains and/or lipid peroxidation end products [6,8,9,12,14,15,39–41]. We found a significant ($p < 0.05^*$) decrease in area of the olefinic band and olefinic═CH/lipid ratio for both PTZ-induced and audiogenetically susceptible groups. It should be noted that, with FTIR spectroscopy one cannot distinguish whether the reduction in the area of olefinic mode is due to a decrease in the concentration of unsaturated lipids or due to lipid peroxidation. The main reason of this reduction can be the release of glutamate throughout epileptic activity activating phospholipases, which use membrane lipids as reservoirs to produce second messengers, prostaglandins and leukrotines, and to enhance further glutamate release [42,43]. During this process, unsaturated lipids are most susceptible to be metabolized since they account for more than 20% of total fatty acids of brain [44]. On the other hand, as a perspective, it has to be mentioned that enhanced oxidative stress and changes in antioxidant capacity, both of which leading to membrane lipid peroxidation, are considered to play an important role in the pathogenesis of epileptic seizures, also shown by several reports in the literature [42,43,45–47]. In addition, it is well-known that when lipid peroxidation increases, the amount of unsaturated lipids, and consequently the area/intensity of olefinic mode decreases [5,9,38,41]. In line with these findings, our results show a reduction in the amount of unsaturated lipids in brain tissue membranes of PTZ-induced and audiogenetically susceptible groups, to which lipid peroxidation may also contribute. There are some mechanisms for the production of the

Table 2
The wavenumber, band area, area ratios and bandwith values of FTIR bands for control, PTZ-treated and audiogenetically susceptible groups for rat brain tissue membranes. The values are the mean ± standard deviation for each sample. The degree of significance was denoted as * on corrected p-values.

Functional group	Control (n = 6)	PTZ-treated (60 mg/kg) (n = 6)	p values	Audiogenetically susceptible (n = 5)	p values
Frequency values					
CH_2 asymmetric	2921.22 ± 1.11	2922.45 ± 0.34	0.129	2924.17 ± 0.53	0.005*
CH_2 symmetric	2851.81 ± 0.37	2852.74 ± 0.44	0.150	2854.70 ± 0.61	0.002*
C═O	1736.09 ± 0.07	1734.72 ± 1.37	0.004*	1732.17 ± 1.39	0.031*
PO^-_2 asymmetric	1236.88 ± 3.45	1232.40 ± 1.15	0.028*	1231.32 ± 0.87	0.039*
PO^-_2 symmetric	1080.92 ± 0.58	1078.92 ± 2.76	0.052	1075.58 ± 2.12	0.033*
Band area					
Olefinic═CH	1.41 ± 0.03	1.25 ± 0.02	0.045*	1.09 ± 0.07	0.039*
CH_2 asymmetric	16.25 ± 0.09	15.25 ± 0.78	0.042*	14.51 ± 1.14	0.011*
C═O	6.41 ± 0.07	5.78 ± 1.37	0.037*	5.06 ± 0.45	0.005*
Amide I	27.47 ± 1.78	26.90 ± 1.23	0.018*	26.01 ± 1.03	0.036*
Amide II	13.27 ± 2.14	11.95 ± 1.01	0.040*	10.47 ± 0.14	0.049*
COO− symmetric	3.99 ± 0.06	3.72 ± 0.34	0.195	2.71 ± 0.19	0.047*
PO^-_2 asymmetric	9.41 ± 0.14	9.06 ± 0.08	0.254	8.78 ± 1.17	0.029*
PO^-_2 symmetric	10.54 ± 0.11	9.75 ± 0.61	0.022*	8.28 ± 0.47	0.033*
Band area ratios					
Olefinic═CH/lipid	0.06 ± 0.006	0.05 ± 0.004	0.019*	0.04 ± 0.002	0.037*
CH_2/lipid	0.62 ± 0.09	0.61 ± 0.02	0.295	0.60 ± 0.11	0.015*
CH_3 asym/lipid	0.33 ± 0.004	0.32 ± 0.001	0.024*	0.31 ± 0.002	0.026*
C═O/lipid	0.28 ± 0.08	0.25 ± 0.17	0.045*	0.22 ± 0.51	0.040*
Lipid/protein	0.59 ± 0.002	0.61 ± 0.001	0.049*	0.63 ± 0.003	0.017*
Bandwidth					
CH_2 asymmetric	13.18 ± 0.07	13.03 ± 0.10	0.290	12.83 ± 0.06	0.011*
CH_2 symmetric	7.09 ± 0.23	6.79 ± 0.14	0.021*	6.43 ± 0.82	0.055*

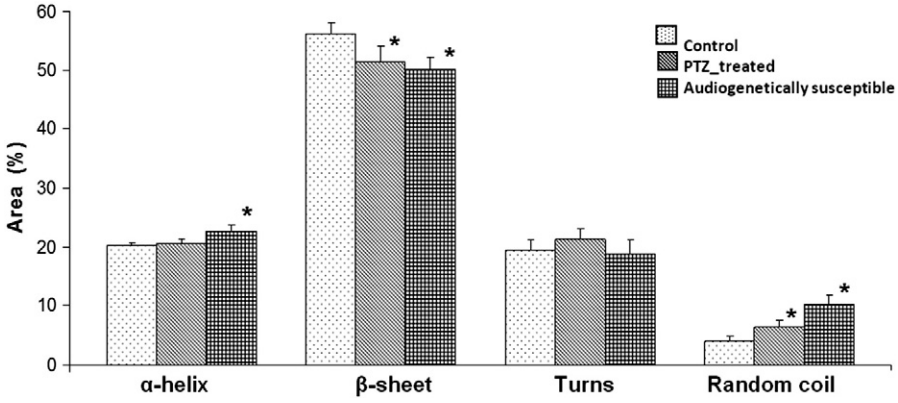

Fig. 3. Bar diagram of protein secondary structural variations for control, PTZ-treated and audiogenetically susceptible groups.

molecules leading to lipid peroxidation throughout epileptic activities. One of such mechanisms is mitochondrial respiratory chain (MRC), which is known as the major source of ROS in cells. The attack of ROS to mitochondrial membrane lipids gives rise to disruption of electron transport chain (ETC) components, resulting in mitochondrial dysfunction. Lipid peroxidation-induced mitochondrial dysfunction during seizures had been already demonstrated [42]. Moreover, same molecules are also generated with metabolism of arachidonic acid (AA) upon the activation of phospholipases with the release of excitatory neurotransmitters [42,43] as mentioned above. In addition, the reduced form of glutathione (GSH), the most effective free radical scavenging compound in the nervous system, was found to be impaired during epileptic conditions as shown by examination of epileptic patients [45].

In addition to a decrease in unsaturated lipid content the lower ratios of CH_2/lipid, C═O/lipid and CH_3 asym/lipid together with a decrease in the CH_2 asymmetric, the C═O, the PO^-_2 symmetric and the PO^-_2 asymmetric and the COO^- symmetric stretching modes areas may have also resulted from the breakdown of already existing membrane lipids [6,7,15,48] or synthesis of lipids in insufficient amount in both treatment groups [48,49]. This situation may be also viewed as an impairment in energy metabolism; since phospholipid synthesis is an energy demanding process depending on mitochondrial function [42,45,49]. Furthermore, c-hydroxybutyric acid (GHB), whose primary precursor is GABA, naturally exists in mammalian brain cell membrane [50]. Since GABA levels in brain are declining throughout epileptic seizures, this could cause low production of GHB at the same time. The decrement in membrane lipids indicates shortened chain lengths, consequently altered lipid composition and distribution [6,9,15,25]. This fact could affect the overall surface charge of the membrane and its interaction with peripheral and integral membrane proteins, might account for altered membrane function as demonstrated for Na/K-dependent ATPase action [51]. On the other hand, the change in lipid profile may represent an imbalance in the distribution of inner and outer leaflets of the bilayer, which further points to lipid

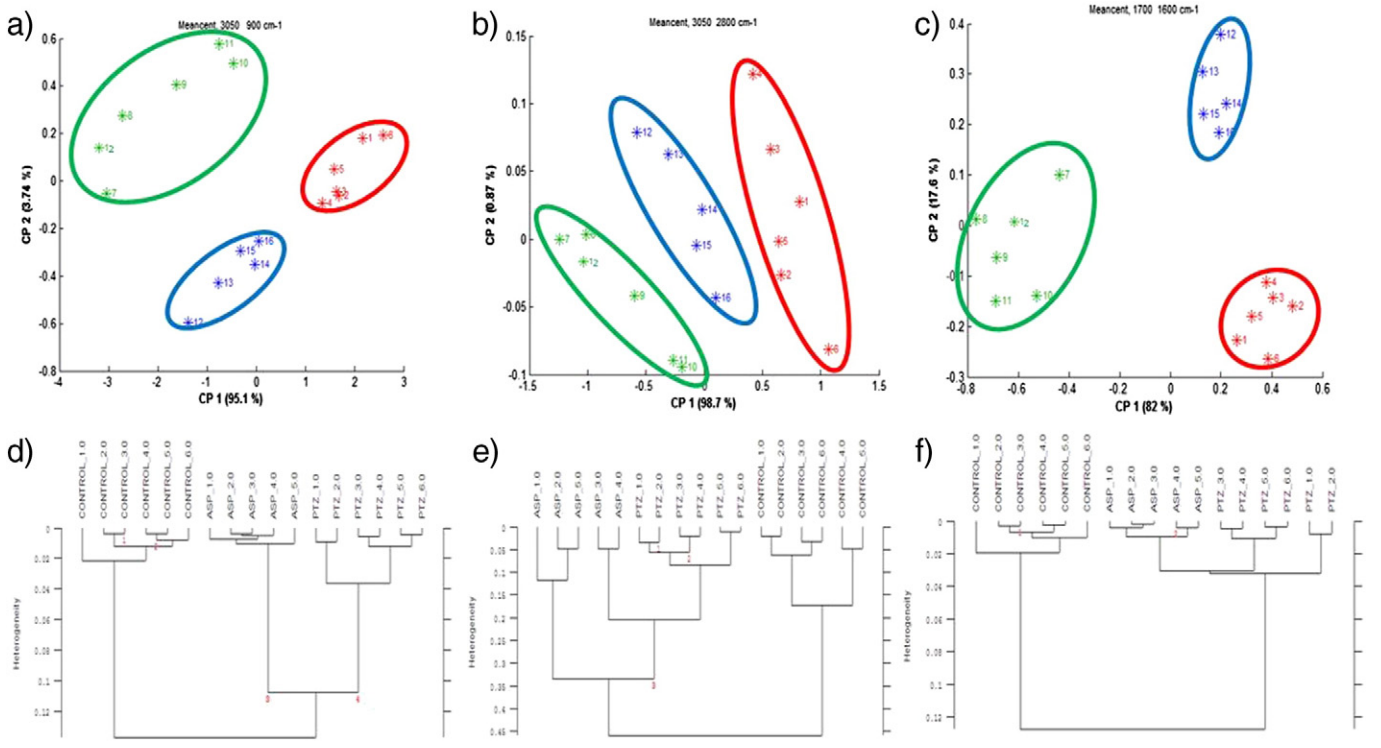

Fig. 4. PCA analysis of the FT-IR spectra of brain tissue membrane in control (red), PTZ (green), and audiogenetically susceptible (blue) groups in (a) 3050–900 cm^{-1}, (b) 3050–2800 cm^{-1}, (c) 1700–1600 cm^{-1} regions. The percentages between brackets represent the proportion of variance held in the principal components. Hierarchial clustering of control, PTZ-treated and audiogenetically groups in the (d) 3050–900 cm^{-1}, (e) 3050–2800 cm^{-1}, (f) 1700–1600 cm^{-1} spectral range. Average absorbance spectra were used to construct the clusters in both methods.

asymmetry. Under this circumstance, it was suggested that there has to be a compensatory change such as variation in membrane curvature and thickness [6,9,52].

Various types of membrane proteins like membrane-bound enzymes, ion channels and receptors are involved in the generation of epileptic seizures that are defined as the result of excessive, abnormal and synchronized nerve cell activity [1]. Among these, integral membrane proteins interact with fatty acyl chains of membrane lipids through hydrophobic matching. In contrast, peripheral membrane proteins are predominantly bound to lipid head groups by electrostatic and hydrogen-bond interactions [15,21,53]. Because of this bilateral association between membrane components, physical properties of host lipid molecules and proteins can mutually impact their conformation, and hence their activity as shown in both model and biological membrane systems [54–56]. In order to gain information about protein structure and chemical features of membrane lipids, which determine their organization and packing within bilayer, we have monitored the frequency changes of the CH_2 asymmetric, the CH_2 symmetric, the C═O, the PO^-_2 asymmetric and symmetric stretching bands. The CH_2 asymmetric and the CH_2 symmetric modes are used to investigate physical state of lipids and membrane order [6,9,25]. A significant change in the positions of the CH_2 bands to higher frequencies for audiogenetically susceptible group indicates a substantial increment in gauche conformers in acyl chains [6,25,57]. This may further cause loose packing of membrane [57,58]. In addition, the shifts in the C═O, the PO^-_2 asymmetric and PO^-_2 symmetric modes to lower wavenumbers, also appeared to be more profound for audiogenetically susceptible group, which imply an increase in the hydration state of the glycerol backbone near the hydrophilic part and polar head group of the membrane lipids. The hydrogen bonding might be between water molecules and the oxygen molecules of both carbonyl and phosphate groups of phospholipids or hydrophilic protein residues [25]. This is likely from the activation of the enzymes that change lipid head group size influencing the area occupied by the lipids [21,52]. All variations in lipid packing may directly affect their interaction with hydrophobic and hydrophilic residues of proteins, and thereby membrane insertion of proteins, which have been shown to especially modulate the cell-lytic properties of alpha helical transbilayer peptide [59]. Accordingly, due interactions of lipids with proteins, the rearrangement of lipids may also result from the changes in structure and topology membrane proteins. For instance, the rough surface of a membrane protein brings about poor packing of acyl chains. Otherwise, a rigid protein surface reduces the motional fluctuations of hydrocarbon chains and forcing them to tilt. Subsequently, lipids become conformationally disordered to maximize contact with the protein, as also investigated by the shifting of CH_2 stretching modes to higher degrees [60]. On the other hand, the packing of membrane lipids in a different manner may affect functions of glycolipids and glycoproteins which may operate as cell receptors and be responsible for cell signaling [61]. All of these changes in membrane lipids, effective in membrane protein conformation and activity, may play a fundamental role for the generation of epileptic seizures.

The elucidation of the conformation of membrane proteins enables structure–function analyses in pathophysiological conditions [1,61–64]. However, membrane proteins are located within hydrophobic environment of the bilayer and they tend to be unstable when extracted. In recent years, NN method has been used to predict protein secondary structure [6,8,15,33]. According to NN results of the presented study, both treatments caused significant changes, as predominantly indicated by a decrease in beta sheet and random coil structures, and a significant increase in alpha helix only for audiogenetically susceptible group (Fig. 3). In particular, the increment in random coil structure represents protein denaturation, leading to dysfunction [5,6,15,25] as also documented for some membrane proteins like glucose transporters and Na/K ATPase in epileptic conditions [1,64]. The significant increase in alpha helix specifically in audiogenetically susceptible group might have resulted from disordered membrane structure as displayed by the frequency changes of CH_2 stretching bands. This might suggest that membrane proteins are forced by such potency of increased surface of fatty acyl chains readily interacting with hydrophobic monomers of membrane spanning domain of proteins, which is mostly alpha helix motif. In a different mechanism, in response to any stimulating factor voltage dependent K^+ channels, acetylcholine receptors and many other transmembrane receptors and ion channels can be clustered [65]. By this way, membrane spanning domains of these proteins are then conformationally altered to stabilize membrane curvature [21,52,54]. Hence, structural changes in proteins together with the altered lipid organization resulted from epileptic seizures may possibly alter membrane dynamics.

FT-IR spectroscopy allows simultaneous investigation of lipid and protein structure and composition, in membrane systems, as overall. Here, we have specifically focused on lipid to protein ratio to detect the variations on the lipid and/or protein asymmetry due to its importance in cellular functions [6,9,37]. The similar approach was performed in our previous studies [5–9,15,25]. An increment in lipid to protein ratio, which is more profound in audiogenetically susceptible group, suggests an increase in lipid content or a decrease of proteins, or both [7,9,15]. We have observed a reduction in both lipid and protein content for both treated groups but the degree of decrement in proteins was higher than that of lipids. The decline in protein content may have arisen from protein degradation due to activation of proteasomes as well as attacks of free radicals [5,15,66,67]. Particularly, these kinds of alterations in raft arrangement may result in the reduced intrinsic anisotropy. Together with the changes in chemical composition of membrane components, altered lipid to protein ratio may give rise to a dynamic instability via the retraction of membrane connection with the intracellular cytoskeletal elements [68]. Such events may account for membrane perturbation and may prove loss of viability, which was correlated with a permanent loss of membrane integrity during epileptic activity [64].

We have found a reduction in lipid fluidity in both treated groups. This finding is in accordance with the study performed on erythrocyte membranes obtained from epileptic patients [69] but not with the reports on other cellular membranes [22–24,70]. In those studies, increased membrane fluidity for subcellular membranes of mitochondria, microsomes, lysosomes and endoplasmic reticulum upon the occurrence of epileptic seizures were reported. These studies were performed with purified membrane systems. However, our results showed a decrease in membrane fluidity. Since we cannot exclude the possibility that our preparation does contain membrane compartments in addition to cell membrane, there is a probability that, cumulatively the fluidity might appear as decreased due to the presence of other membrane compartments in addition to cell membrane. Decrease in fluidity might have various consequences. Double bonds in unsaturated lipids cause the formation of kinks which force the molecules further apart and allow for more movement. But, the low content of these lipids might have led to the loss of freedom of motion in membranes. Additionally, an increase in cholesterol/phospholipid ratio [71], rigid surfaces of membrane proteins [60] and the formation of cross-linking between the lipid-lipid and protein-lipid moieties [9,15] can be mentioned as reasons for less fluid lipids. Lipid fluidity is strictly controlled for proper functioning of membrane receptors, since it is involved in providing energetic constraints to select for certain membrane proteins with adapted trans-membrane segments [72]. Thus, a lowered membrane fluidity found in the current study can be another indication of functional changes of membrane proteins.

Based on their spectral variations, all groups analyzed were successfully discriminated in the region of 3050–2800 cm^{-1}, 1700–1600 cm^{-1} and 3050–900 cm^{-1}. Three distinct clusters in PCA and cluster analysis corresponding to control and treated groups refer to the epileptic activities induced by PTZ injection and audiogenetical stimulation leading to significant variations in brain membranes in terms of the content, structure and composition of membrane components. Particularly, 100%

value for specificity and sensitivity for both treated groups revealed that the variations found in brain tissue membranes have potential to generate precondition for the development and expression of seizures even if they are triggered by different stimuli.

In order to reduce the occurrence of epileptic seizures, antiepileptic drugs are developed to act on the elements playing role in excessive neuronal firing. Therefore, most of the therapeutic strategies of antiepileptic drugs are focused on stabilizing the membrane, increasing GABAergic transmission, decreasing excitatory amino acid transmission and prevention of depolarization by acting on ion channels [73]. The structure and proper functioning of brain membrane compartments are important in the maintenance of the equilibrium in neuronal communication. In neuronal networks, direct or indirect modulation of antiepileptic agents has potential to normalize the disruption in membrane systems which might lead to imbalanced excitation and inhibition.

5. Conclusion

Our findings suggest that both types of epileptic convulsions cause several alterations in the molecular content, structure and function of brain tissue membrane that may contribute to the stimulation of epileptic activity. In particular, a decrease in lipid and protein content, and membrane fluidity were observed. We have also found a significant change in lipid packing, which is pivotal in membrane curvature. Additionally, an altered structural profile for membrane proteins was predicted with an increase in random coil whereas a decrease in beta sheet in both treatment groups. In summary, our findings showing compositional and structural changes detected by FT-IR spectroscopy and predicted with NN analysis indicate possible membrane based factors playing important roles in the generation of epileptic activities.

Acknowledgement

This study is supported by the Scientific Research Foundation (BAP) of Middle East Technical Universiy and Scientific and Technical Research Council of Turkey (SBAG-2940-104S475).

References

[1] G. Avanzini, S. Franceschetti, Cellular biology of epileptogenesis, Lancet Neurol. 2 (2003) 33–42.
[2] R.J. De Lorenzo, D.A. Sun, L.S. Deshpande, Cellular mechanisms underlying acquired epilepsy: the calcium hypothesis of the induction and maintenance of epilepsy, Pharmacol. Ther. 105 (2005) 229–266.
[3] M. Dastgheib, L. Moezi, Acute and chronic effects of agomelation on intravenous penthylenetetrazol-induced seizure in mice and the probable role of nitric oxide, Eur. J. Pharmacol. 736 (2014) 10–15.
[4] K. Sarkivosa, G. van Luijtelaar, Prog. Neuro-Psychopharmacol. Biol. Psychiatry (2001), http://dx.doi.org/10.1016/j.pnpbp.2010.11.010.
[5] A. Dogan, K. Ergen, F. Budak, F. Severcan, Evaluation of disseminated candidiasis on an experimental animal model: a Fourier transform infrared study, Appl. Spectrosc. 61 (2007) 199–203.
[6] G. Cakmak, F. Zorlu, M. Severcan, F. Severcan, Screening of protective effect of amifostine on radiation-induced structural and functional variations in rat liver microsomal membranes by FT-IR spectroscopy, Anal. Chem. 83 (2011) 2438–2444.
[7] N. Toyran, F. Zorlu, G. Donmez, K. Oge, F. Severcan, Chronic hypoperfusion alters the content and structure of proteins and lipids of rat brain homogenates: a Fourier transform infrared spectroscopy study, Eur. Biophys. J. Biophys. Lett 33 (2004) 549–554.
[8] O. Bozkurt, S.H. Bayari, M. Severcan, C. Krafft, J. Popp, F. Severcan, Structural alterations in rat liver proteins due to streptozotocin-induced diabetes and the recovery effect of selenium: Fourier transform infrared microspectroscopy and neural network study, J. Biomed. Opt. 17 (7) (2012) 076023.
[9] N. Ozek, B. Bal, Y. Sara, R. Onur, F. Severcan, Structural and functional characterization of simvastatin-induced myotoxicity in different skeletal muscles, BBA-Gen. Subj. 406 (2014) 406–415.
[10] R. Fiorini, G. Curatola, E. Bertoli, P.L. Giorgi, A. Kantar, Changes of fluorescence anisotropy in plasma membrane of human polymorphonuclear leukocytes during the respiratory burst phenomenon, FEBS Lett. 273 (1990) 122–126.
[11] H.H. Mantsch, R.N. McElhaney, Phospholipid phase transitions in model and biological membranes as studied by infrared spectroscopy, Chem. Phys. Lipids 3 (1991) 213–226.
[12] F. Severcan, G. Gorgulu, S. Turker Gorgulu, T. Guray, Rapid monitoring of diabetes-induced lipid peroxidation by Fourier transform infrared spectroscopy: evidence from rat liver microsomal membranes, Anal. Biochem. 339 (2005) 36–40.
[13] C. Petibois, G. Deleris, Chemical mapping of tumor progression by FT-IR imaging: towards molecular histopathology, Trends Biotech. 24 (2006) 455–462.
[14] F. Severcan, O. Bozkurt, R. Gurbanov, G. Gorgulu, FT-IR spectroscopy in diagnosis of diabetes in rat animal model, J. Biophotonics 3 (2010) 621–626.
[15] S. Turker, G. Ilbay, M. Severcan, F. Severcan, Investigation of compositional, structural, and dynamical changes of pentylenetetrazol-induced seizures on a rat brain by FT-IR spectroscopy, Anal. Chem. 86 (2014) 1395–1403.
[16] J. Chwiej, J. Dulinska, K. Janeczko, P. Dumas, D. Eichert, J. Dudala, Z. Setkowicz, Synchrotron FT-IR micro-spectroscopy study of the rat hippocampal formation after pilocarpine-evoked seizures, J. Chem. Neuroanat. 40 (2) (2010) 140–147.
[17] J. Dudala, K. Janeczko, Z. Setkowicz, J. Chwiei, The use of SR-FT-IR microspectroscopy for a preliminary biochemical study of the rat hippocampal formation tissue in case of pilocarpine induced epilepsy and neuroprotection with FK-506, Nukleonika 52 (2012) 615–619.
[18] J. Kutorasinska, Z. Setkowicz, K. Janeczko, C. Sandt, P. Dumasi, J. Chwiei, Differences in the hippocampal frequency of creatine inclusions between the acute and latent phases of pilocarpine model defined using synchrotron radiation-based FT-IR microspectroscopy, Anal. Bioanal. Chem. 405 (2013) 7337–7345.
[19] S. Garip, D. Sahin, F. Severcan, Epileptic seizures-induced structural and functional changes in rat femur and tibia bone tissues: a Fourier transform infrared imaging study, J. Biomed. Opt. 18 (11) (2013) 111409.
[20] S. Kumar, V. Kumar, D.C. Gain, Fourier transform infrared spectroscopic studies on epilepsy, migrane and paralysis, IJE Trans. B 75 (2010) 363–369.
[21] J.M. Boggs, Lipid molecular hydrogen bonding: influence on structural organization and membrane function, BBA-Rev. Biomembr. 906 (1987) 353–404.
[22] M.M. Acharya, S.S. Katyare, Picrotoxin-induced convulsions alters rat brain microsomal membrane structural properties, Neurosci. Lett. 394 (1) (2006) 9–12.
[23] M.M. Acharya, S.S. Katyare, Structural and functional alterations in mitochondrial membrane in picrotoxin-induced epileptic rat brain, Exp. Neurol. 192 (2005) 79–88.
[24] M.M. Acharya, S.H. Khamesra, S.S. Katyare, Picrotoxin-induced convulsions and lysosomal function in rat brain, Ind. J. Clin. Biochem. 20 (2005) 56–60.
[25] S.B. Akkas, S. Inci, F. Zorlu, F. Severcan, Melatonin affects the order, dynamics and hydration of brain membrane lipids, J. Mol. Struct. 834–836 (2007) 207–215.
[26] R.J. Racine, Modification of seizure activity by electrical stimulation. 2. Motor seizure, Electroencephalogr. Clin. Neurophysiol. 32 (1972) 1039–1049.
[27] L.V. Vinogradova, Audiogenic kindling in WAG/Rij rats: change in behavioral and electrophysiological responses to repetitive short acoustic stimulation, Zh. Vyssh. Deiat. Im. I. P. Pavlova 54 (2004) 638–647.
[28] Y. Dobryakova, V. Dubynin, G. van Luijtelaar, Maternal behavior in a genetic animal model of absence epilepsy, Acta Neurobiol. Exp. 68 (2008) 502–508.
[29] L. Scott, M.J. Schell, A.L. Hubbard, Isolation of plasma membrane sheets and plasma membrane domains from rat liver. Biomembrane protocols. I. Isolation and analysis", in: J. Graham, J. Higgins (Eds.), Methods in Molecular Biology, Humana Press, Totowa, NJ, 1993, pp. 59–69.
[30] S. Yoon, A. Kazusaka, S. Fujita, FT-IR spectroscopic and HPLC chromatographic studies of carbon tetrachloride induced acute hepatitis in rats: damage in liver phospholipid membrane, Biopolym. Biospectroscopy 57 (2000) 267–271.
[31] G. Birarda, G. Grenci, L. Businaro, B. Marmiroli, S. Pacor, F. Piccirilli, L. Vaccari, Infrared microspectroscopy of biochemical response of living cells in microfabricated devices, Vib. Spec. 53 (2010) 6–11.
[32] A. Naumann, G. Heine, R. Rauber, Fields Crop Res. 119 (2010) 78–84.
[33] M. Severcan, P.I. Haris, F. Severcan, Using artificially generated spectral data to improve protein secondary structure prediction from Fourier transform infrared spectra of proteins, Anal. Biochem. 332 (2) (2004) 238–244.
[34] H.S. Chen, S. Lipton, The chemical biology of clinically tolerated NMDA receptor antagonists, J. Neurochem. 97 (2006) 1611–1626.
[35] H.A. Andree, C.P.M. Reutelingsperger, R. Hauptmann, H.C. Hemker, W.T. Hermens, G. M. Willems, Binding of vascular anticoagulant to planar phospholipid bilayer, J. Biol. Chem. 265 (1990) 4923–4928.
[36] M.S. Awayda, W. Shao, F. Guo, M. Zeidel, W.G. Hill, ENaC–membrane ınteractions regulation of channel activity by membrane order, J. Gen. Physiol. 123 (2004) 709–727.
[37] B. Szalontai, Y. Nishiyama, Z. Gombos, N. Murata, Membrane dynamics as seen by Fourier transform infrared spectroscopy, Biochim. Biophys. Acta 1509 (2000) 409–419.
[38] A. Leskovjan, A. Kretlow, L. Miller, Fourier transform infared imaging shows reduced unsaturated lipid content in hippocampus of a mouse model of Alzheimer disease, Anal. Chem. 82 (2010) 2711–2716.
[39] D. Moore, R. Sills, R. Mendelsohn, Peroxidation of erythrocytes: FT-IR spectroscopy studies of extracted lipids, isolated membranes, and intact cells, Biospectroscopy 1 (2) (1995) 133–140.
[40] K. Liu, R. Bose, H.H. Mantsch, Infrared spectroscopic study of diabetic platelets, Vib. Spectrosc. 28 (2002) 131–136.
[41] R.H. Sills, D.J. Moore, R. Mendelsohn, Erythrocyte peroxidation-quantitation by Fourier transform infrared-spectroscopy, Anal. Biochem. 218 (1994) 118–123.
[42] H.R. Cock, X. Tong, I.P. Hargreaves, S.J.R. Heales, J.B. Clark, P. Patsalos, M. Thom, M. Groves, Mitochondrial dysfunction associated with neuronal death following status epilepticus in rat, Epilepsy Res. 48 (2002) 157–168.
[43] J. Niquet, R.A. Baldwin, S.G. Allen, D. Fujikawa, C.G. Wasterlain, Hypoxic neuronal necrosis: protein synthesis-independent activation of A cell death program, Proc. Natl. Acad. Sci. 100 (2003) 2825–2830.
[44] M. Bourre, Roles of unsaturated fatty acids (especially omega-3 fatty acids) in the brain at various ages and during ageing, J. Nutr. Health Aging 8 (3) (2004) 163–174.

[45] B. Sutter, O. Schrötterner, Advances in Epilepsy Surgery, Springer Wien, New York, 2002.
[46] N. Patsoukis, G. Zervoudakis, C.D. Georgiou, Thiol redox state and lipid and protein oxidation in the mouse striatum after pentylenetetrazol-induced epileptic seizure, Epilepsia 46 (2005) 1205–1211.
[47] M.I. Bellissimo, D. Amado, D. Abdalla, E. Ferreir, E. Cavalheiro, Superoxide dismutase, glutathione peroxidase activities and the hydroperoxide concentration are modified in the hippocampus of epileptic rats, Epilepsy Res. 46 (2001) 121–128.
[48] X. Ma, G. Liu, S. Wang, Z. Chen, M. Lai, Z. Liu, J. Yang, Evaluation of sphingolipids changes in brain tissues of rats with pentylenetetrazol-induced kindled seizures using MALDI-TOF-MS, J. Chromatogr. B 859 (2007) 170–177.
[49] R. Cenedella, C. Sarkar, Mechanism of depression of brain phospholipid levels by an epileptogenic drug, Biochem. Pharm. 33 (1984) 591–598.
[50] O. Snead, R. Furner, C. Liu, In vivo conversion of ã-aminobutyric acid and 1,4-butanediol to ã-hydroxybutyric acid in rat brain: studies using stable isotopes, Biochem. Pharm. 38 (1989) 4375–4380.
[51] G.Y. Sun, A. Sun, Phospholipids and acyl groups of synaptosomal and myelin membranes isolated from the cerebral cortex of squirrel monkey (Saimiri sciureus), Biochim. Biophys. Acta 22 (1974) 15–18.
[52] T. Harvey, L. Gallop, Membrane curvature and mechanisms of dynamic cell membrane remodelling, Nature 438 (2005) 590–596.
[53] G. Brasseur, T. Pillot, L. Lins, J. Vandekerckhove, M. Rosseneu, Peptides in membranes: tipping the balance of membrane stability, Trends Biochem. Sci. 22 (1997) 167–171.
[54] P. Yeagle, The Structure of Biological Membranes, CRC Press, Boca Raton, FL, 1992.
[55] H. Sandermann, Biochim. Biophys. Acta 515 (1978) 209–237.
[56] R.N. McElhaney, in: S. Razin, S. Rottem (Eds.), Current Topics in Membranes and Transport, vol. 17, Academic Press, New York, 1982.
[57] L. Senak, R. Mendelsohn, CH_2 wagging modes as quantitative ır probes of acyl chain conformational order in phospholipid-membranes, Biophys. J. 64 (1993) A299-A299.
[58] G. Saberwal, R. Nagaraj, Cell-lytic and antibacterial peptides that act by perturbing the barrier function of membranes: facets of their conformational features, structure-function correlations and membrane-perturbing abilities, Biochim. Biophys. Acta Rev. Biomembr. 1197 (1994) 109–131.
[59] C. Stefaniu, G. Brezesinski, H. Möhwald, Langmuir monolayers as models to study processes at membrane surfaces, Adv. Colloid Interf. Sci. 208 (2014) 197–213.
[60] W. Curatolo, Glycolipid function, Biochim. Biophys. Acta 906 (1987) 137–160.
[61] S. Lin, H. Chu, Fourier transform ınfrared spectroscopy used to evidence the prevention of beta-sheet formation of amyloid beta (1–40) peptide by a short amyloid fragment, Int. J. Biol. Macromol. 32 (2003) 173–177.
[62] M. Apetri, N. Maiti, M. Zagorski, P. Carey, V. Anderson, Secondary structure of α-synuclein oligomers: characterization by raman and atomic force microscopy, J. Mol. Biol. 355 (1) (2006) 63–71.
[63] D. Janigro, Blood–brain barrier, ion homeostasis and epilepsy: possible implications towards the understanding of ketogenic diet mechanisms, Epilepsy Res. 37 (1999) 223–232.
[64] E. Farge, D. Ojcius, A. Subtil, A. Dautry-Varsat, Enhancement of endocytosis due to aminophospholipid transport across the plasma membrane of living cells, Am. J. Physiol. 276 (1999) C725–C733.
[65] M. Jackson, B. Ramjiawan, M. Hewko, H.H. Mantsch, Infrared microscopic functional group mapping and spectral clustering analysis of hypercholesterolemic rabbit liver cell, Mol. Biol. 44 (1998) 89–98.
[66] M.T. Curtis, D. Gilfor, J.L. Farber, Lipid-peroxidation ıncreases the molecular order of microsomal-membranes, Arch. Biochem. Biophys. 235 (1984) 644–649.
[67] M. Lokar, D. Kabaso, N. Resnik, K. Sepcic, A. Iglic, The role of cholesterol-sphingomyelin membrane nanodomains in the stability of intercellular membrane nanotubes, Int. J. Nanomedicine 7 (2012) 1891–1902.
[68] A. Tangorra, G. Curatola, E. Bertoli, Evaluation of antiepileptic drug effect on membrane fluidity, Exp. Mol. Pathol. 55 (1991) 180–189.
[69] M. Patel, Mitochondrial dysfunction and oxidative stress: cause and consequence of epileptic seizures, Free Radic. Biol. Med. 37 (2004) 1951–1962.
[70] W.L. Hubbell, H.M. McConnell, Molecular motion in spin-labeled phospholipids and membranes J, Am. Chem. Soc. 93 (1971) 314.
[71] J.X. Lu, S. Sharpe, R. Ghirlando, W.M. Yau, Oligomerization state and supramolecular structure of the HIV-1 Vpu protein transmembrane segment in phospholipid bilayers, Protein Sci. 19 (2010) 1877–1896.
[72] M. Mantegazza, G. Curia, G. Biagini, D. Ragsdale, M. Avoli, "Voltage gated sodium channels as therapeutic targets in epilepsy", THE Lancet, Neurology 9 (2010) 413–424.
[73] K. Hammond, M. Reboiras, I. Lyle, N. Jones, Characterisation of phosphatidylcholine/phosphatidylinositol sonicated vesicles. Effects of phospholipid composition on vesicle size, Biochim. Biophys. Acta 774 (1984) 19–25.